Precise SHRIMP U-Pb zircon age constraints on the lower Waterberg and Soutpansberg Groups, South Africa

H.C. Dorland, N.J. Beukes, J. Gutzmer
Paleoproterozoic Mineralization Research Group, Department of Geology, University of Johannesburg,
PO Box 524, Auckland Park, 2006, South Africa
e-mail: HCDorland@yahoo.com; njb@rau.ac.za, jg@rau.ac.za

D.A.D. Evans
Department of Geology and Geophysics, Yale University, New Haven, Connecticut, USA
e-mail: dai.evans@yale.edu

R.A. Armstrong
Research School of Earth Sciences, Australian National University, Canberra, Australia
e-mail: Richard.Armstrong@anu.edu.au

ABSTRACT

Erosional remnants of Paleoproterozoic red bed successions such as the Olifantshoek, Soutpansberg, Waterberg and Palapye Groups cover an extensive area of the Kaapvaal Craton. Depositional ages of these successions have been ill-defined and their lateral correlation a subject of controversial debate. We report precise zircon SHRIMP U-Pb ages of 2054 ± 4 and 2051 ± 8 Ma for quartz porphyry lavas stratigraphically near the base of the Waterberg Group from the Lower Swaershoek and correlative Rust de Winter Formations. The Entabeni Granite, erosively overlain by the Soutpansberg Group, yields a precise zircon SHRIMP age of 2021 ± 5 Ma. These ages indicate that at least part of the Waterberg Group is older than the Soutpansberg Group. In addition, the lower part of the Waterberg Group was deposited immediately after intrusion of the Bushveld Complex and may be tectonically related to the complex.

Introduction

Voluminous late Paleoproterozoic red bed successions, including the Waterberg, Soutpansberg, Palapye, and Olifantshoek Groups, and the Shoshong and Blouberg Formations (Jansen, 1976; 1982; Meinster, 1977; Key, 1983; Cheney *et al.*, 1990; Callaghan *et al.*, 1991; Carney *et al.*, 1994; Bumby *et al.*, 2001) cover large parts of the Archean Kaapvaal Craton and parts of the Limpopo Metamorphic Complex in geographically and tectonically separated outcrop areas in southern Africa (Figure 1). Although the successions have often been correlated based on lithostratigraphic and sequence-stratigraphic comparisons (Jansen, 1976; Cheney and Twist, 1986; Cheney *et al.*, 1990), the correlations have not been rigorously tested by high-precision geochronology. Of special interest are the stratigraphic relations and depositional ages of the Waterberg and Soutpansberg Groups. Early workers correlated these successions primarily on the basis of post-Bushveld (~2058 Ma) unmetamorphosed red-bed lithologies (Crockett and Jones, 1975; Jansen, 1976; Barker, 1983). In contrast, Cheney *et al.* (1990) argued that the Soutpansberg Group is older than the Waterberg Group, whereas Bumby *et al.* (2001) suggested the opposite. Much of this controversy arises from a dearth of precise age constraints from the two successions.

Early attempts at geochronology among the Waterberg and Soutpansberg Groups yielded imprecise results. Whole-rock Rb-Sr ages of 1749 ± 104 Ma and 1769 ± 34 Ma for hydrothermally altered lava flows and sills from the Sibasa Formation (Barton, 1979), and a Pb-Pb whole-rock age that defines an imprecise secondary isochron of 1809 + 263/-317 Ma for the same samples (Cheney *et al.*, 1990) are the only available geochronological data for the Soutpansberg Group. A similar age of 1790 ± 90 Ma, calculated with obsolete decay constants, was reported from a thin porphyritic lava in the Rust de Winter Formation (Oosthuyzen and Burger, 1964), considered an outlier of the basal succession of the Waterberg Group (Cheney and Twist, 1986). However, more recent U-Pb determinations showing greater precision and concordance illustrate that these earlier Rb/Sr and Pb/Pb ages most probably reflect later alteration events and cannot be used to constrain formation ages. For example, Hanson *et al.* (2004) obtained U-Pb age for baddeleyite of 1927.3 ± 0.7 Ma and 1878.8 ± 0.5 to 1873.7 ± 0,8 Ma from dolerite intruding the lower and upper parts of the Waterberg Group respectively, indicating deposition of at least part of that succession prior to ~1.97 Ga.

We augment the high-precision geochronological database here with concordant SHRIMP U-Pb zircon ages of quartz porphyry lava in the Rust de Winter and Lower Swaershoek Formations (Jansen, 1970; 1982) of the Waterberg Group. In addition, we provide a new precise single zircon age for the post-tectonic Entabeni Granite in the Southern Marginal Zone of the Limpopo Complex. This granite is unconformably overlain by

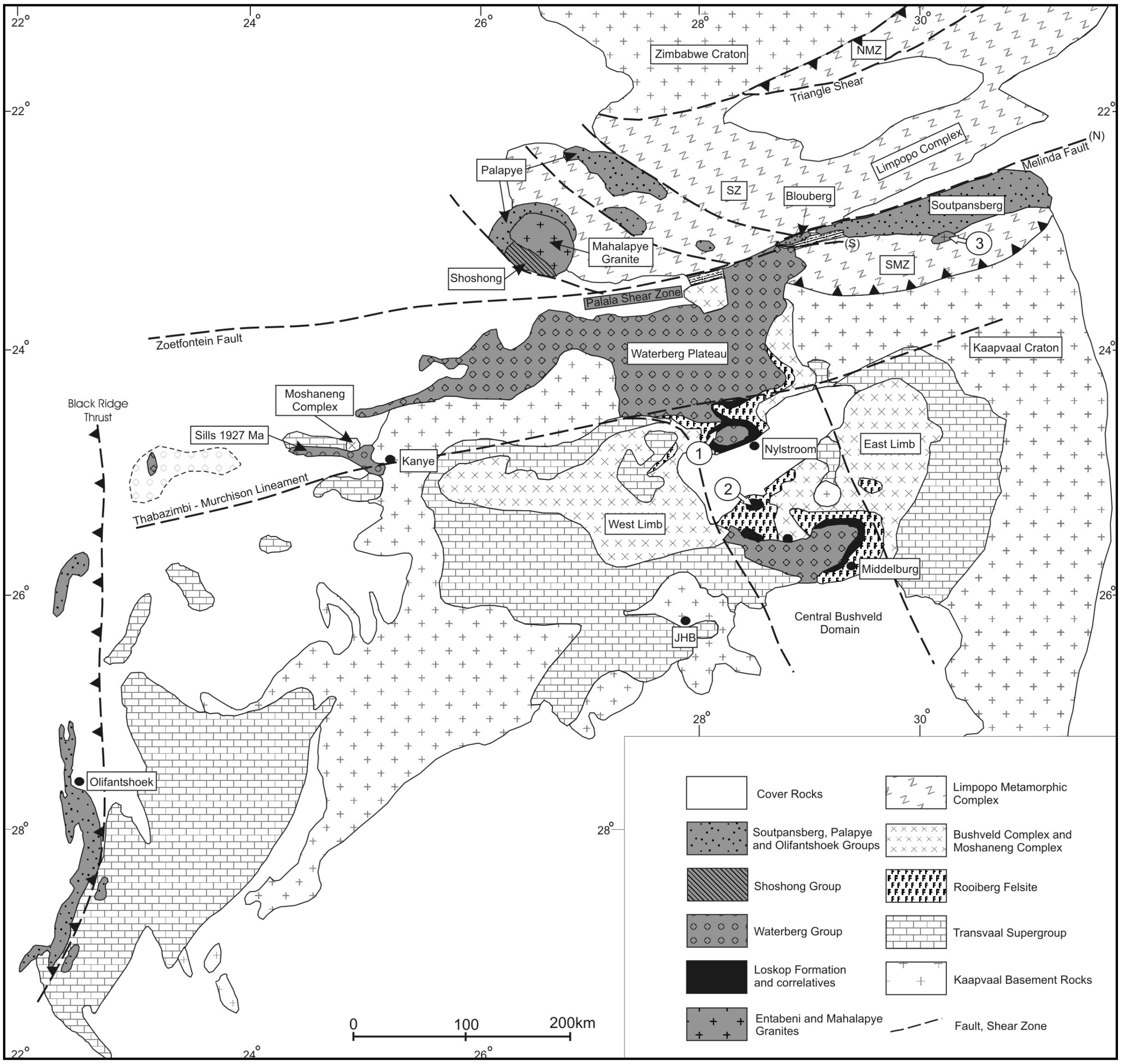

Figure 1. Map showing the distribution of the Paleoproterozoic red bed successions in northern South Africa and eastern Botswana. Location of samples dated are numbered: 1 = Quartz porphyry lava, Lower Swaershoek Formation, Nylstroom syncline, 2 = Quartz porphyry lava of Rust de Winter Formation, 3 = Entabeni Granite. N and S refer to northern and southern strands of the Melinda Fault in the Blouberg area. Jhb = Johannesburg.

the Soutpansberg Group and the age thus provides a lower limit for deposition of that succession. Previously, the Entabeni Granite was dated at 1957 ± 3 Ma, but the zircon data have large discordance (Barton *et al.*, 1995).

Geological Setting

Structural Domains of Red Beds

The Paleoproterozoic red bed successions of northern South Africa and eastern Botswana are preserved in four distinct fault-bounded structural domains (Figure 1) resulting in uncertainties of correlation from one domain to the other. The Waterberg Group is preserved on the Kaapvaal Craton to the south of the Zoetfontein-Melinda Fault that represents re-activated structures along the Palala Shear Zone forming the southern boundary of the Central Zone of the Limpopo Metamorphic Complex. The Soutpansberg Group is preferentially preserved along the extension of the Palala Shear Zone and unconformably overlies mylonites of the shear zone and granulite-facies metamorphic rocks of the Southern Marginal Zone of the Limpopo Complex (Figure 1). This succession is separated from the main outcrop area of the Waterberg Group to the south by the southern strand of the Melinda fault. To the north it is bounded by the northern strand of the Melinda fault. Locally, in the Blouberg area (Figure 1), the Waterberg Group is unconformably overlain by the Soutpansberg Group between the northern and southern strands of the Melinda Fault (Bumby *et al.*, 2001).

To the northwest of the Soutpansberg Group, the Palapye Group (Mapeo *et al.*, 2004) overlies high-grade metamorphic rocks and post-tectonic Mahalapye granite of the Central Zone of the Limpopo Complex (Figure 1). The strata are preserved due to faulting along major arcuate shear zones that tangentially merge with the Palala Shear Zone (Figure 1).

In contrast to the Waterberg, Soutpansberg and Palapye Groups, which are little deformed, the Olifantshoek Group (Figure 1) in Northern Cape Province is intensely folded. It is essentially in an allochthonous position because it is preserved in the hanging wall to the west of the Black Ridge Thrust. Autochthonous strata of the Olifantshoek Group are only preserved in small areas to the east in the footwall of the thrust.

Waterberg Group

The Waterberg Group is a mildly deformed succession of red beds preserved in two main structural domains on the Kaapvaal Craton, namely a) an east-west elongated domain bounded by the Zoetfontein-Melinda Faults in the north and the Thabazimbi-Murchison Lineament in the south and b) a north-northwest elongated domain situated between the eastern and western lobes of the Bushveld Complex termed the Central Bushveld domain (Figure 1). The domain between the Zoetfontein Fault and Thabazimbi-Murchison Lineament comprises the main outcrop area of the Waterberg Group, known as the Waterberg Plateau area, and two smaller outcrop areas to the west of Kanye in eastern Botswana (Figure 1). The Central Bushveld domain comprises the Nylstroom syncline outcrop area of the Waterberg Plateau and the Middelburg area (Figure 1). In addition there are a number of small erosional outliers between Middelburg and Nylstroom, the largest of which is at Rust de Winter (Figure 1).

The type area for the Waterberg Group is in the Waterberg Plateau and here it is represented by an ~5 km thick red bed succession of conglomerate, quartzite and shale with minor volcanics especially in its lower part (Figure 2). The lithostratigraphic subdivision of the Waterberg Group is complex with different formation names used

(a) among the various structural domains,
(b) for the same stratigraphic unit across the border between South Africa and Botswana, and
(c) within a specific rock unit to indicate lateral facies changes (SACS, 1980; Jansen, 1982; Carney *et al.*, 1994).

This rather confusing situation has been largely clarified by Cheney and Twist (1986) who recognized five major unconformity-bounded sequences (WUBS I-V) in the Waterberg Plateau area (Figure 3A) and extended these sequences to other outcrop areas (Figure 3B). The quartz porphyry lava samples dated in this study come from the Rust de Winter and Lower Swaershoek Formations which form part of the basal unconformity-bounded sequence (WUBS I). According to Cheney and Twist (1986), WUBS I also incorporates both the Glentig Formation in the Waterberg Plateau area and the Loskop Formation, which underlies the Wilgerivier Formation with a marked angular unconformity in the Middelburg area (Figures 3A and 3B).

In broad terms WUBS I is characterized by a mixed red bed succession of conglomerate, quartzite and shale with subordinate felsic volcanics including the quartz porphyry lavas dated in this study (Figure 2). WUBS I everywhere directly overlies felsic volcanic rocks of the Rooiberg Group (Figure 1), with an age of 2061 ± 2 Ma (Walraven, 1997). It paraconformably overlies the felsites, which immediately preceded the intrusion of the mafic phase of the Bushveld Complex at ~2.06 Ga (Walraven, 1997), and never contains pebbles of Bushveld granite. Such pebbles are common from

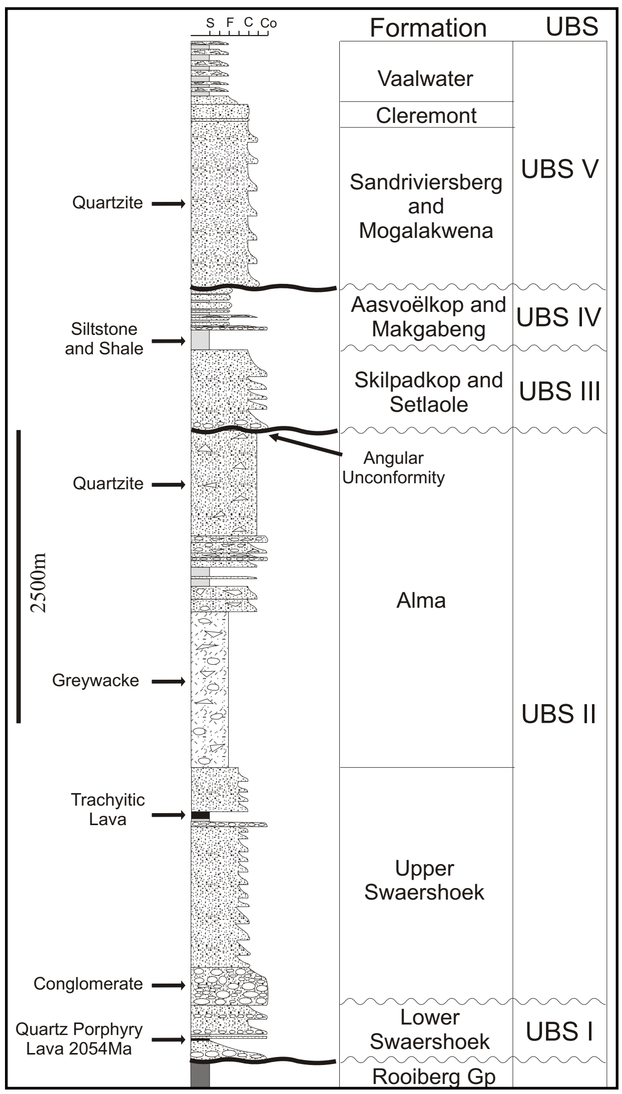

Figure 2. Stratigraphy of the Waterberg Group in its type area of the Waterberg Plateau (modified after Jansen, 1982). Also shown is the subdivision of the succession into five unconformity-bounded sequences after Cheney and Twist (1986). Grain size scale: S = shale, F = fine sand, C = coarse sand, Co = conglomerate.

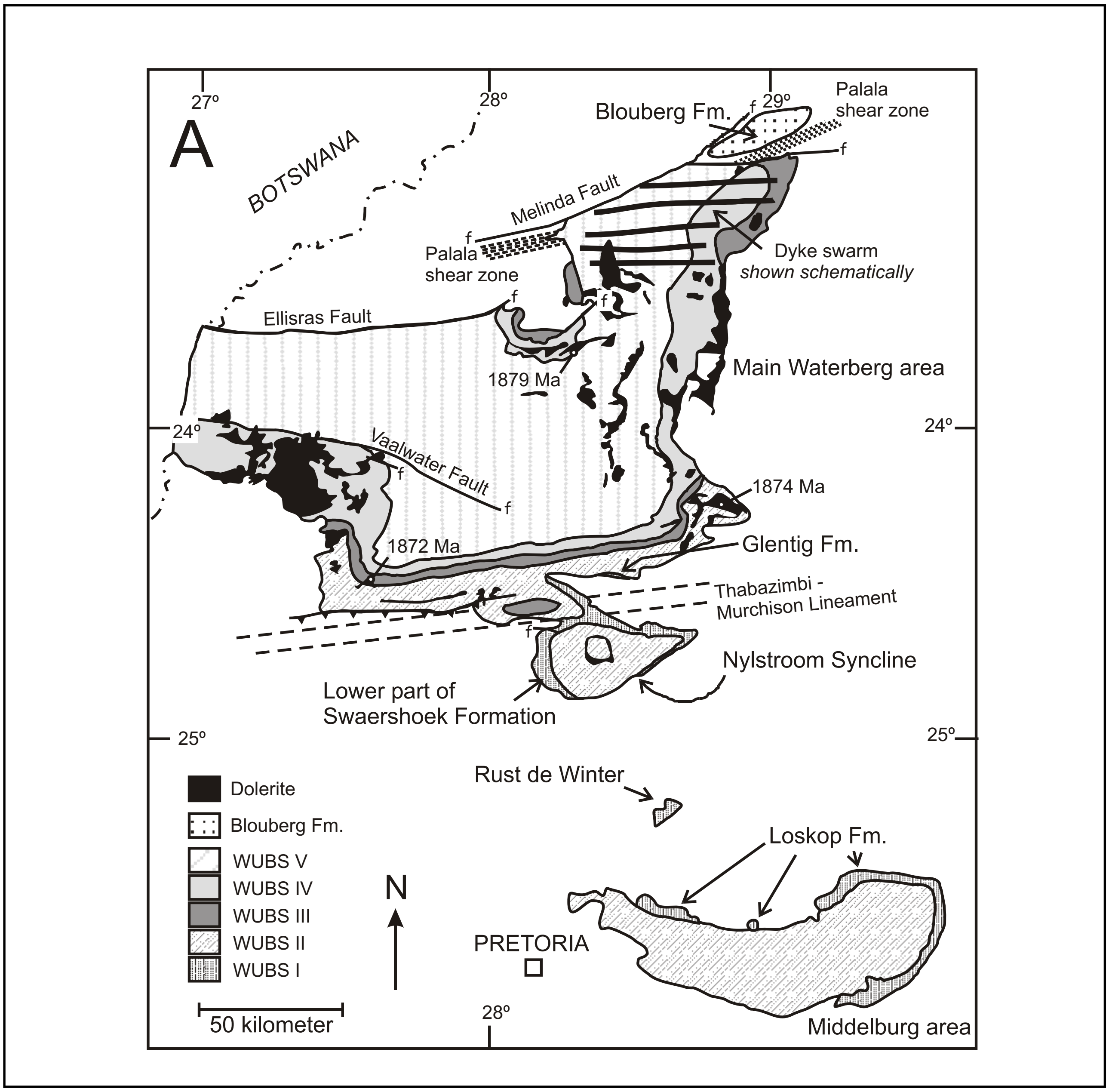

Figure 3. (**A**) Distribution of the five unconformity-bounded sequences of the Waterberg Group (modified after Cheney and Twist, 1986). Also shown schematically are the distribution of sills dated by Hanson *et al.* (2004) and the dolerite swarm described by Bumby *et al.* (2001) to the south of Blouberg.

WUBS II upwards in the Waterberg Group (Cheney and Twist, 1986). Based on these stratigraphic relationships, it has been suggested that the deposition of WUBS I preceded intrusion of the Bushveld Complex (Cheney and Twist, 1986). Regionally WUBS I is restricted to the north-northwest-trending Central Bushveld domain, erosively preserved below the regional low-angle unconformity at base of WUBS II (Figures 1 and 3).

Entabeni Granite and Soutpansberg Group

The Soutpansberg Group (Jansen, 1976; Barker, 1983; Bumby, 2001) is exposed in two separate areas, namely the extensive Soutpansberg Mountain Range and the much smaller Blouberg Mountain (Figure 1). In the Soutpansberg Mountain Range the strata generally dip and young to the north, such that along the southern foothills of the range the Soutpansberg Group is in depositional contact with granitoid and metamorphic rocks of the Southern Marginal Zone of the Limpopo Complex. It is here that the succession unconformably overlies a small undeformed granite pluton, known as the Entabeni Granite (Du Toit, 1979; Cheney *et al.*, 1990; Barton *et al.*, 1995) (Figure 1). This granite has been sampled in the present study to obtain a precise lower age limit for deposition of the Soutpansberg Group.

In broad terms the Soutpansberg Group comprises two major unconformity bounded sequences (Cheney *et al.*, 1990). The lower one (SUBS I) is composed of a

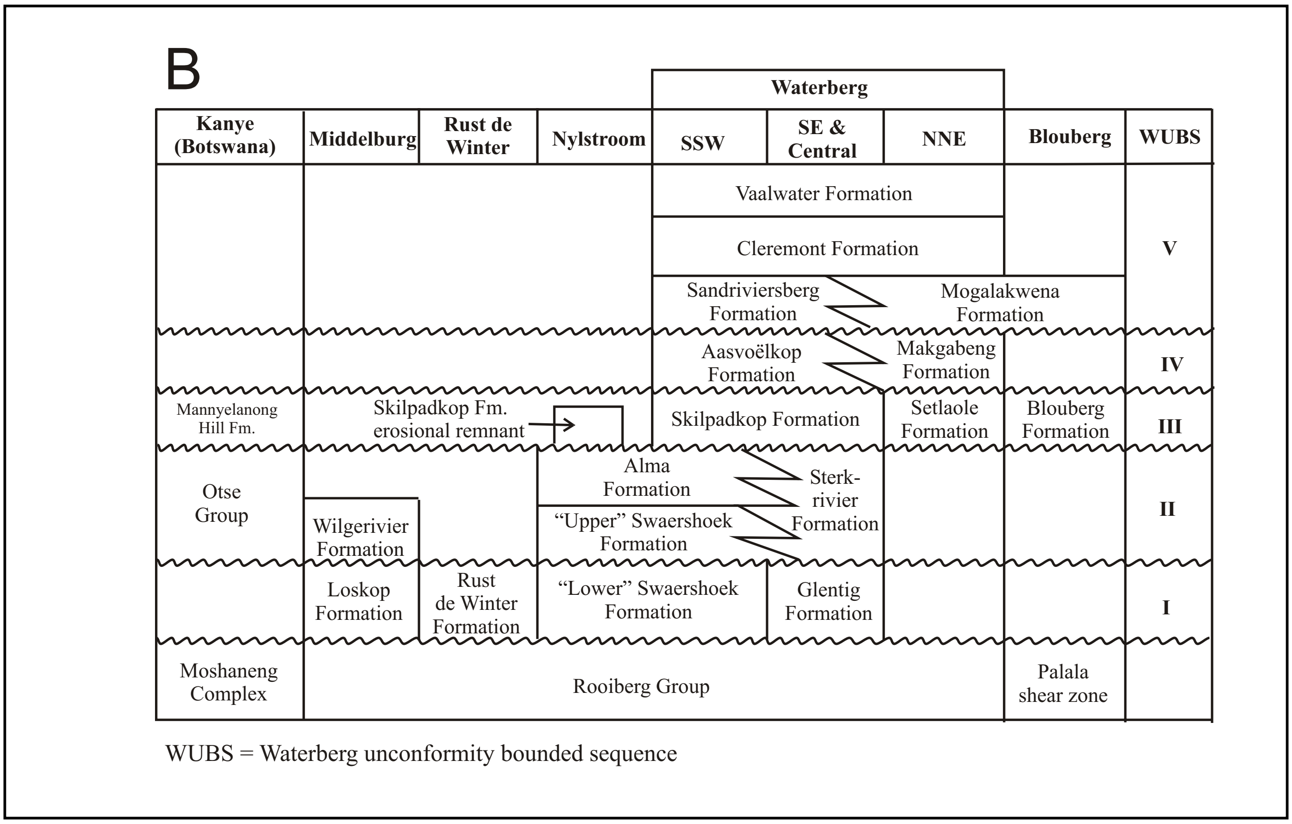

Figure 3. (**B**) Subdivision and correlation of the unconformity-bounded sequences of the Waterberg Group (modified after Cheney and Twist, 1986 and Hanson *et al.*, 2004).

thin (less than 10 m thick) basal conglomerate, quartzite and shale unit known as the Tshifhefhe Formation. It is conformably overlain by the Sibasa Basalt, which is up to 3000 m thick, and the Fundudzi Formation, made up of light grey to purple and red quartzite and conglomerate with interbeds of shale and mafic volcanics, and reaching a maximum thickness of ~1900m (Figure 4). The lower part of the upper unconformity-bounded sequence (SUBS II) is formed by white to purplish quartzite with minor conglomerate of the up to 1500 m thick Wyllies Poort Formation, which is in turn overlain by basaltic lava, shale and quartzite of the Nzhelele Formation (SACS, 1980) with a preserved thickness of ~1000 m (Figure 4).

For purpose of this paper, it is important to note that strata of the Soutpansberg Group are separated from the type succession of the Waterberg Group in the Waterberg Plateau area by the southern strand of the Melinda Fault (Figure 1). Different workers have correlated strata in various ways across the fault. This has led to the controversy of whether the Soutpansberg Group is older (Meinster, 1977; Cheney *et al.*, 1990) or younger (Jansen, 1976; Bumby *et al.*, 2001) than the Waterberg Group.

Sampling Localities

Quartz Porphyry Lava of the Waterberg Group

Quartz porphyry lava from the Lower Swaershoek Formation (WUBS I of Cheney and Twist, 1986) was sampled on Rhenosterpoort 402 KR to the west of Nylstroom at 24° 39' 18.7" S and 28° 10' 28.3" E (Figure 5A). In this area very coarse to granular and pebbly, red quartzite of the Lower Swaershoek Formation rests with sharp erosional, but para-conformable, contact on rhyolite of the Schrikkloof Formation of the Rooiberg Group (Figures 5A and 6). The basal quartzite of the Lower Swaershoek Formation fines upward into a brick-red shale. Lenticular flows of quartz porphyry lava are developed immediately below the shale in the transition zone to the basal quartzite. The porphyry lava flows, of which the petrography and geochemistry are described by Jansen (1970), are not more than a few meters thick. The shale above the lava flows is in turn overlain by quartzite with minor conglomerate, followed by a very thick cobble to boulder conglomerate bed. The latter conglomerate bed has a sharp erosive base and is considered the base of WUBS II in the area (Figure 6).

A second quartz porphyry lava flow was sampled in the Rust de Winter area (Figure 3) on Rust de Winter 180 at 25° 15' 30.1" S and 28° 39' 09.3" E (Figure 5B). At this locality, quartzite and granulestone of the Rust de Winter Formation (Walraven, 1981) overlies rhyolite of the Selonsrivier Formation, the stratigraphic equivalent of the Schrikkloof Formation (SACS, 1980) of the Rooiberg Group. The basal part of the Rust de Winter Formation is composed of approximately 80 m of conglomerate and quartzite (Figure 6). A 3 m-thick, sheet-like flow of quartz porphyry lava overlies this basal conglomerate and quartzite unit. There are virtually no contact

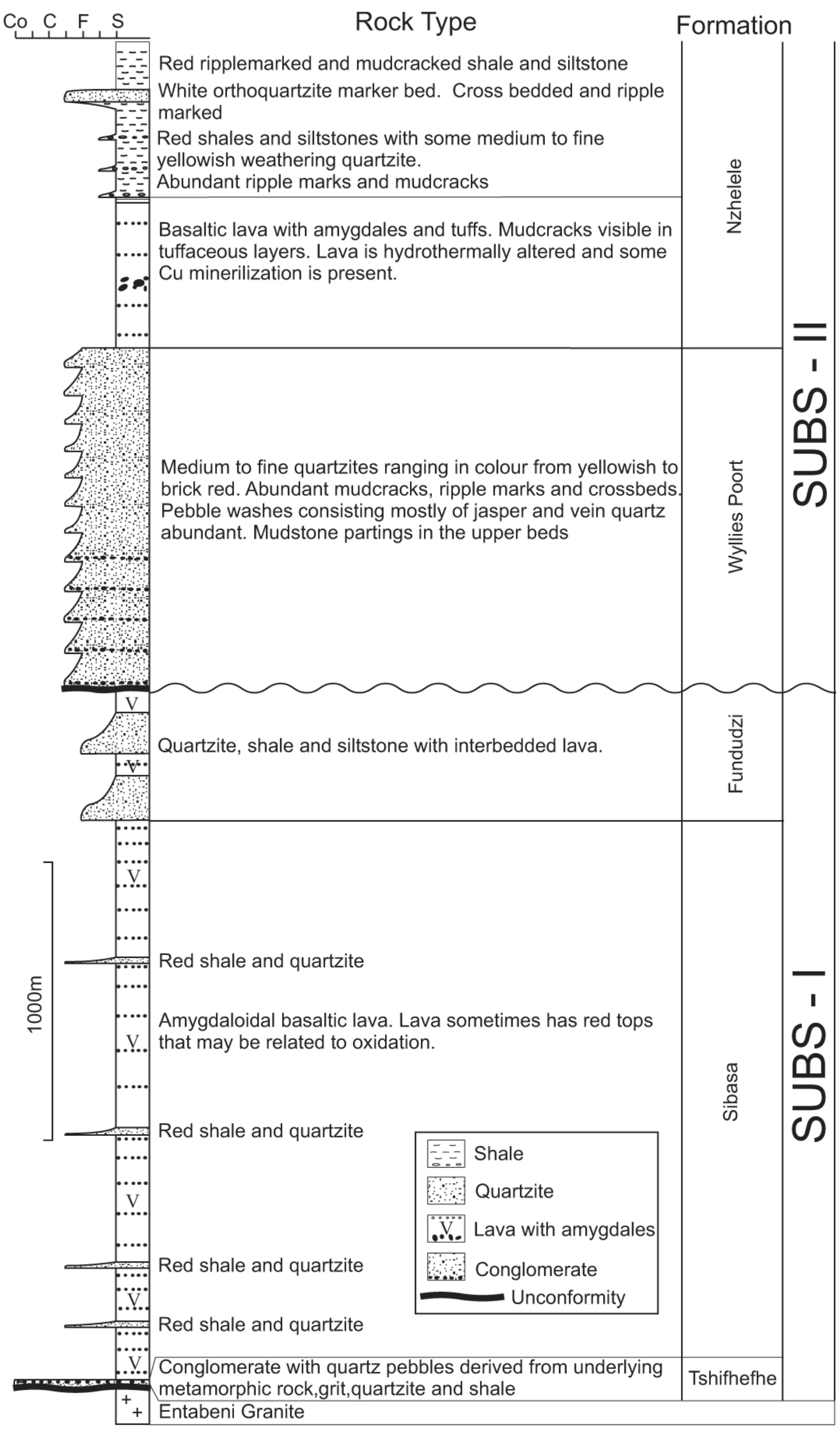

Figure 4. Stratigraphic subdivision and unconformity-bounded sequences of the Soutpansberg Group (modified after SACS, 1980). Grain-size notation similar to that of Figure 2.

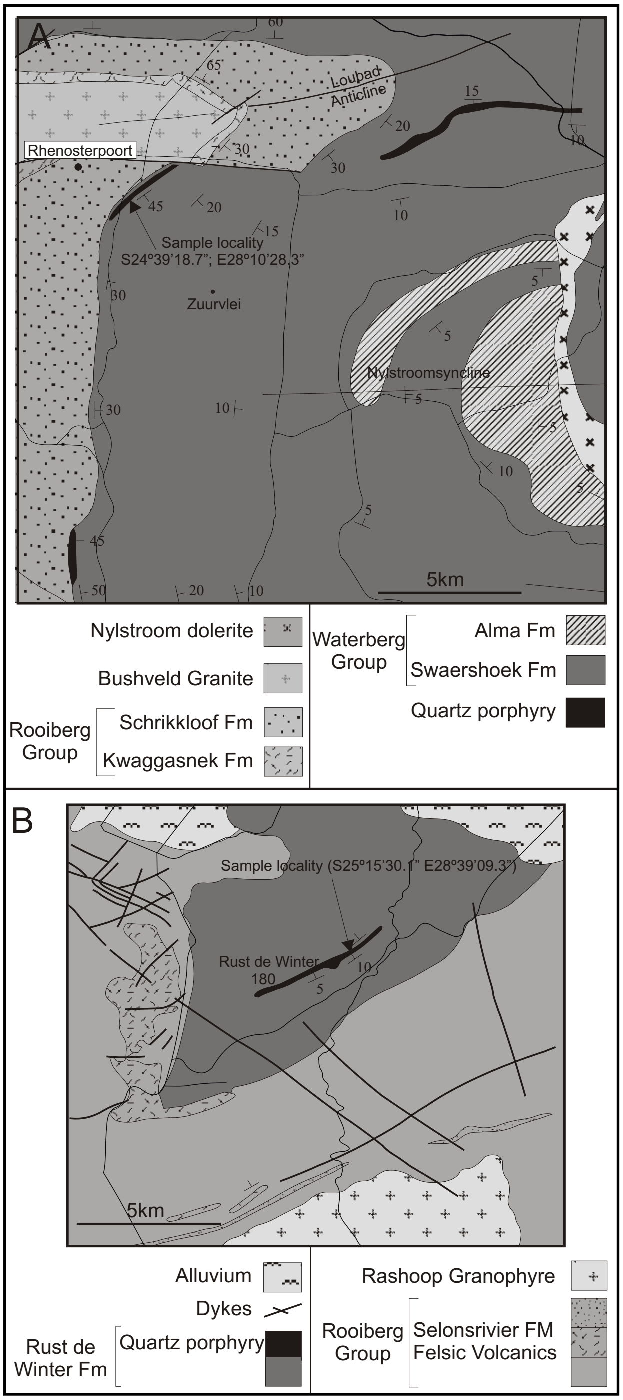

Figure 5. Location maps for samples of the quartz porphyry lava of the Lower Swaershoek Formation (**A**) and the Rust de Winter Formation (**B**).

metamorphic effects on the quartzite at the base of the quartz porphyry lava. The lowermost 5-10 cm of the lava are very fine-grained and may represent devitrified volcanic glass (Glatthaar, 1956). Spherulites are developed in the groundmass of the quartz porphyry, confirming that it is extrusive rather than intrusive in origin (De Bruyn and Andrew, 1972). Quartz porphyry from the same area has previously yielded whole-rock U-Pb ages of 1790 ± 90 Ma (Oosthuyzen and Burger, 1964, with obsolete decay constants) and discordant U-Pb zircon ages of between ~2.06 and ~1.97 Ga (Walraven, 1981).

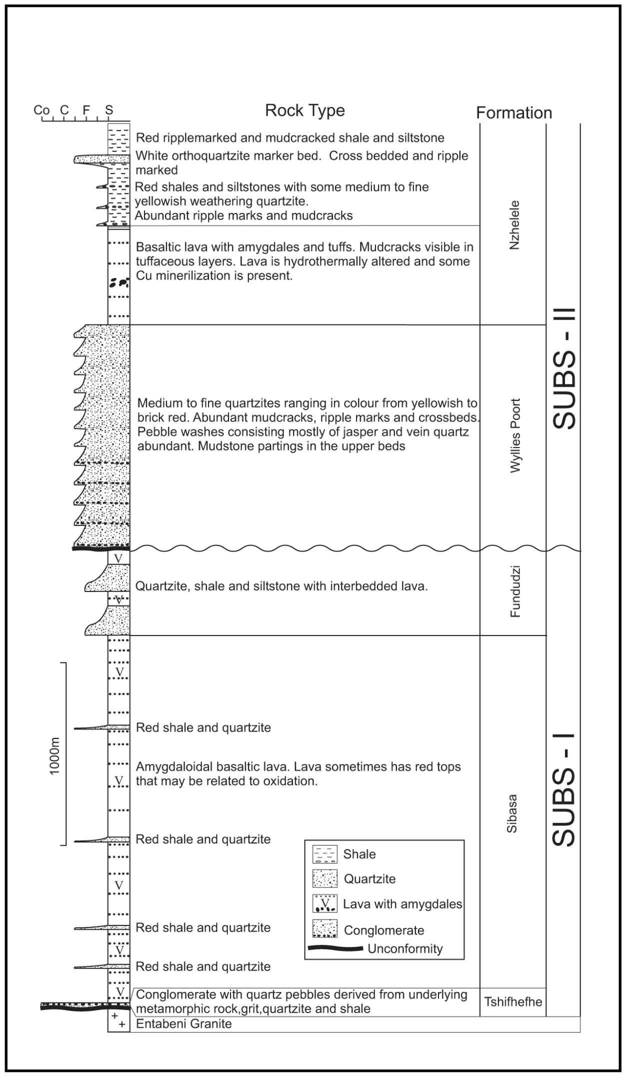

Figure 6. Stratigraphic setting of quartz porphyry lava samples dated from near the base of the Waterberg Group at Rust de Winter and in the Nylstroom syncline. Grain-size notation similar to that of Figure 2.

Quartz porphyry lava flows, of similar composition to those in the lower parts of the Rust de Winter and Swaershoek Formations, are also present in the Glentig Formation to the north of Nylstroom (Figure 3A) and could be equivalent to felsic lavas of the Loskop Formation near Middelburg (Coertze *et al.*, 1977; Jansen, 1982). This is one of the arguments used by Cheney and Twist (1986) to suggest that these successions all correlate with the Lower Swaershoek Formation, *i.e.* WUBS I (Figure 3B).

It is of interest to note that trachytic lava flows are present in the upper part of the Swaershoek Formation (WUBS II) at several localities in the Nylstroom syncline (Jansen, 1970) (Figure 6). Various attempts to separate zircons from these lavas exposed on Driefontein 378 were unsuccessful, despite the fact that some of them contained more than 500 ppm Zr. It is possible that the Zr is present as baddeleyite or zirconolite, and it is suggested that future attempts should focus on extracting these minerals from the trachytic lavas for isotopic dating.

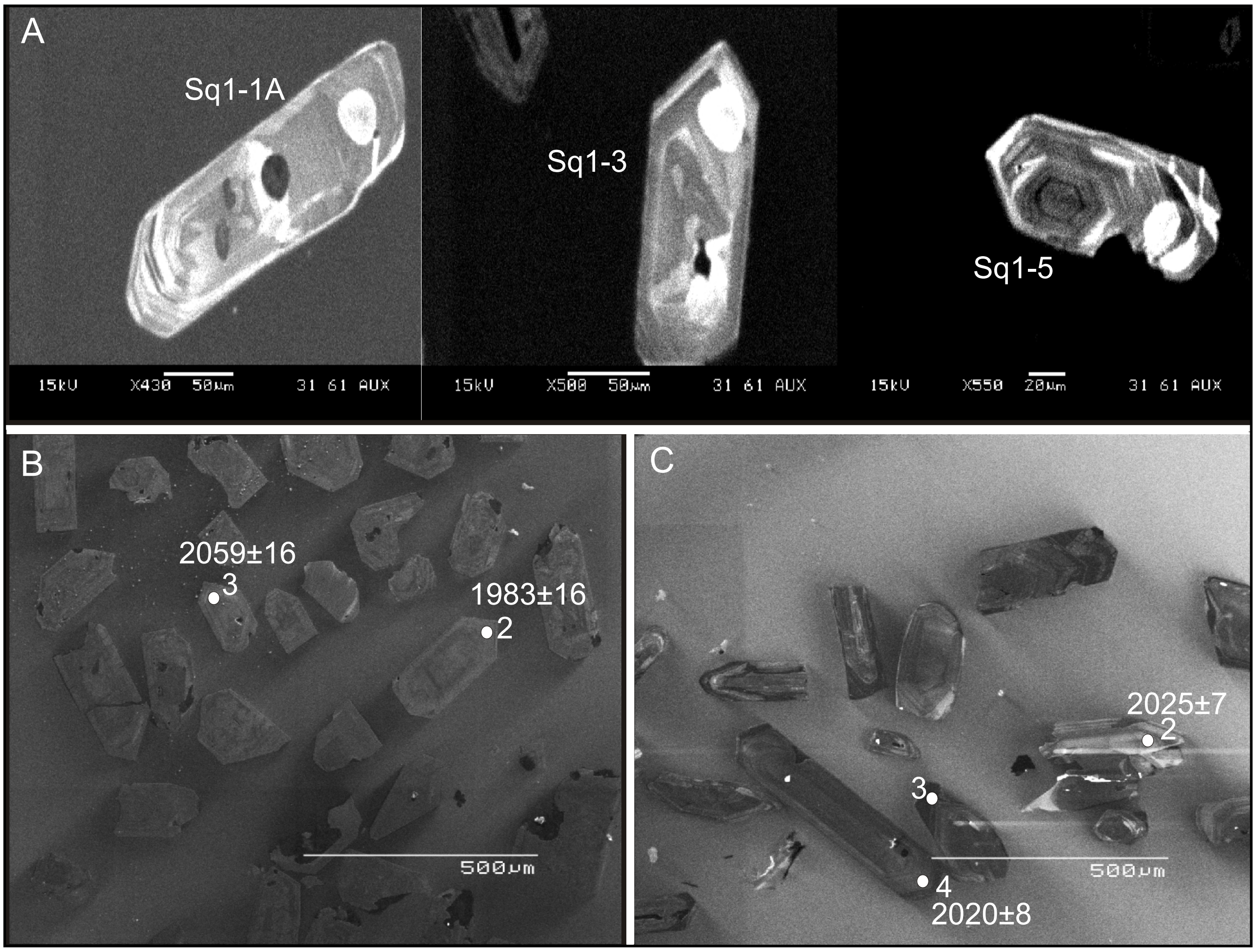

Figure 7. Examples of zircon grains dated by SHRIMP, from the Lower Swaershoek (**A**) and Rust de Winter (**B**) quartz porphyry lavas, and from the Entabeni Granite (**C**).

Entabeni Granite

The Entabeni Granite is a small undeformed, peraluminous two-mica, alkali granite which intrudes high-grade metamorphic and granitoid rocks of the Southern Marginal Zone of the Limpopo Complex (Figure 1). Because of its apparently undeformed nature the granite is considered anorogenic (Du Toit, 1979) or post-tectonic in origin. Petrographic and geochemical descriptions of the granite are provided by Cheney *et al.* (1990) and Barton *et al.* (1995). It is reported to have a composite zircon U-Pb age of 1957 ± 3 Ma (Barton *et al.*, 1995), but the high precision of the age belies a large (32% and 37%) degree of isotopic discordance of the two composite zircon samples. This age is within error of the 1974 ± 14 Ma age obtained from Rb-Sr data on muscovite in the granite (Cheney *et al.*, 1990). For the present study, the Entabeni Granite was sampled in a fresh road cut at 23° 02' 22.9" S and 30° 13' 02.4" E near the Timbadola Saw Mill.

Geochronology

Methods

Samples were prepared using facilities at the Department of Geology at the University of Johannesburg. Hand-samples were first cut with a diamond saw to remove weathered surfaces and then washed and dried before they were disaggregated in a jaw crusher and powdered in a Siebtechnik swing mill. Powdered samples were split in order to obtain representative aliquots of approximately 2 to 2.5 kg from which zircons were separated using standard heavy-liquid and magnetic mineral separation techniques. The zircons were then mounted, polished and photographed, followed by carbon coating and scanning electron microscope cathodoluminescence studies to determine internal texture and zonation of grains. Based on the photomicrographs and cathodoluminescence images, individual zircon grains were selected for analyses by SHRIMP using the procedure described by Compston *et al.* (1984).

SHRIMP analyses of zircons of the Swaershoek quartz porphyry were performed at Curtin University of Technology in Perth, Australia, while zircons from the Rust de Winter quartz porphyry and Entabeni Granite were analyzed at the Australian National University (ANU) in Canberra, Australia. At Curtin University, the CZ3 zircon standard (564 Ma; $206Pb/^{238}U=0.0914$) with a precision (1σ) better than 1% was used for calibration purposes. Initial Pb correction for the total Pb in each analysis was done by removing initial ^{206}Pb, ^{207}Pb and ^{208}Pb, using the observed 204Pb and assuming Pb of

Broken Hill isotopic composition (Cumming and Richards, 1975). Common Pb among the zircon grains is low enough so that the results are not significantly affected by the choice of common Pb models. Errors are expressed at a 95% confidence level. At ANU, zircon grains were mounted in epoxy discs with chips of SL13 zircon standard. The Pb/U ratios were normalized to a value of 0.0928 for the $^{206}Pb/^{238}U$ ratio of the SL13 standard, equivalent to an age of 572 Ma. Analytical data were reduced in a manner similar to that described by Compston *et al.* (1992) and Williams and Claesson (1987).

Results

Zircon grains extracted from the Lower Swaershoek quartz porphyry are on average 150 μm in length, euhedral, prismatic and oscillatory-zoned (Figure 7A); with the typical appearance of zircons from acid igneous rocks. None of the grains showed any signs of rounding or reworking. The cores and rims of 42 grains were analyzed (Table 1); thirty nine of these analyses are nearly concordant (Figure 8A). In combination, they give a ^{204}Pb-corrected $^{207}Pb/^{206}Pb$ age of 2054 ± 3.5 Ma (Figure 8A). This age is thought to represent the best estimate for the extrusion of the porphyritic lava of the Swaershoek Formation.

Zircons from the Rust de Winter quartz porphyry are on average 200 μm in length, euhedral and prismatic in form and oscillatory-zoned (Figure 7B). None of the grains showed any signs of rounding or reworking. The cores and rims of 17 zircon grains from the Rust de Winter porphyry were analyzed; 11 of these yielded nearly concordant to concordant ages (Table 2, Figure 8B). The six most concordant grains (within 2% discordancy) were used to determine a concordia age of 2051 ± 8 Ma, which we consider to represent the best estimate for extrusion of the Rust de Winter porphyry.

Zircon grains of the Entabeni Granite are mostly euhedral and display homogeneous as well as oscillatory-zoned internal structures (Figure 7C). Eighteen analyses were performed on 16 different grains (Table 3). Core and rim ages for the two grains that were analyzed at two spots are within error of one another (Table 3). Most of the grains have a U content of 200 to 400 ppm (Table 3), unlike the grains that were analysed by Barton *et al.* (1995) that were reported to contain more than 800 ppm U. Of the 18 analyses, 16 yielded nearly concordant ages (within 6% discordancy). In combination, they give a $^{207}Pb/^{206}Pb$ age of 2021 ± 5 Ma (Table 3, Figure 8C), which we regard as the best estimate for the crystallization age of the Entabeni Granite.

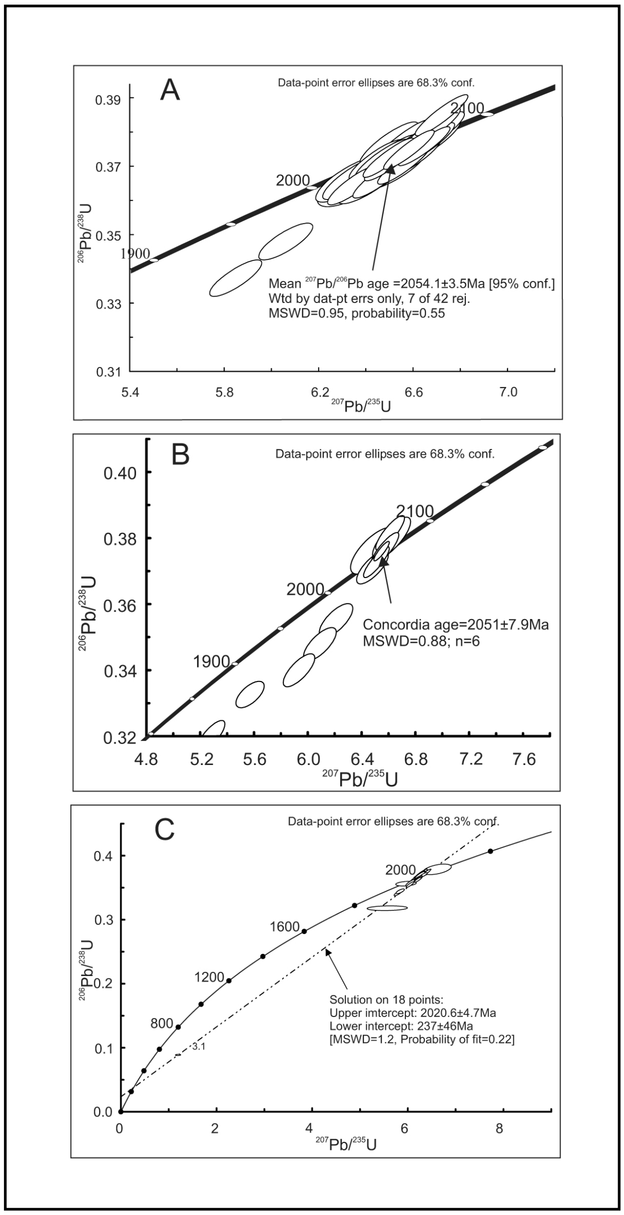

Figure 8. Concordia plots for zircons from quartz porphyry lava of the Lower Swaershoek (**A**) and Rust de Winter (**B**) Formations of the Waterberg Group and of the Entabeni Granite (**C**).

Discussion

Bushveld magmatism versus Waterberg sedimentation

Isotopic ages for the Bushveld Complex suggest emplacement of the mafic-ultramafic suite at ca.2058 Ma (Walraven *et al.*, 1990, Walraven, 1997; Buick *et al.*, 2001), and the granitic suite (Nebo Granite) at 2054 ± 2 Ma (zircon Pb/Pb evaporation, Walraven and Hattingh, 1993). Isotopic ages of 2054 ± 4 Ma and 2051 ± 8 Ma for the respective Swaershoek and Rust de Winter quartz porphyries are within error of the granitic phase of the Bushveld Complex, and are slightly younger than the mafic-ultramafic phase. These results now lead to the conclusion that deposition of the lowermost unconformity-bounded sequence of the Waterberg Group (WUBS I) took place concurrently with or immediately after the emplacement of the granitic phase of the Bushveld Complex (Figure 9). The synchronism of the ages of the porphyritic lavas in the Nylstroom and Rust de Winter areas also supports their stratigraphic correlation and the interpretation that they belong to the same unconformity-bounded sequence (WUBS I)

Table 1. Summary of SHRIMP U-Pb data for zircons from the quartz porphyry lava of the "Lower" Swaershoek Formation.

Grain.Spot	(1)	ppm	ppm	$^{232}Th/^{238}U$	ppm	(1)		(1)		%	(1)	±%	(1)	±%	(1)	±%	errcorr
	%	U	Th		$^{206}Pb^*$	$^{206}Pb/^{238}U$		$^{207}Pb/^{2206}Pb$		Discordant	$^{207}Pb^*/^{206}Pb^*$		$^{207}Pb^*/^{235}U$		$^{206}Pb^*/^{238}U$		
	$^{206}Pb_c$					Age		Age									
11.1	0.02	99	40	0.41	31.2	2,018	±19	2,039	±13	1	0.12574	0.74	6.375	1.3	0.3677	1.1	0.833
22.1	0.03	89	34	0.4	27.9	2,008	±20	2,060	±14	3	0.12722	0.78	6.412	1.4	0.3655	1.2	0.829
23.1	0.1	79	41	0.53	25	2,011	±20	2,033	±15	1	0.1253	0.87	6.324	1.5	0.3661	1.2	0.803
24.1	0.09	163	90	0.57	51	2,004	±18	2,047	±10	2	0.12628	0.57	6.349	1.2	0.3646	1	0.879
25.1	0.08	164	84	0.53	52.4	2,038	±18	2,038	±11	0	0.12568	0.61	6.444	1.2	0.3719	1	0.863
26.1	–	124	72	0.6	39.3	2,031	±19	2,070	±11	2	0.12798	0.64	6.535	1.3	0.3704	1.1	0.861
27.1	0.13	125	48	0.4	39.4	2,013	±19	2,035	±12	1	0.12544	0.68	6.339	1.3	0.3665	1.1	0.849
28.1	–	176	76	0.44	55.4	2,014	±18	2,066	±9.3	3	0.12769	0.53	6.455	1.2	0.3666	1	0.892
29.1	–	217	101	0.48	69.5	2,041	±18	2,048	±8.0	0	0.12641	0.45	6.493	1.1	0.3725	1	0.914
210.1	0.02	111	47	0.44	35.1	2,026	±19	2,041	±12	1	0.12586	0.7	6.409	1.3	0.3693	1.1	0.845
211.1	0	69	26	0.39	22.2	2,046	±21	2,056	±15	0	0.1269	0.87	6.536	1.5	0.3735	1.2	0.811
212.1	–	249	97	0.4	80.3	2,052	±18	2,061	±7.7	0	0.1273	0.43	6.579	1.1	0.3749	1	0.918
213.1	–	170	80	0.49	54.5	2,048	±18	2,057	±9.6	0	0.12701	0.55	6.551	1.2	0.374	1	0.887
214.1	0.05	134	54	0.42	43	2,043	±19	2,065	±11	1	0.12761	0.62	6.563	1.2	0.373	1.1	0.867
215.1	0.05	88	28	0.33	28.1	2,027	±20	2,069	±15	2	0.1279	0.85	6.514	1.4	0.3695	1.1	0.804
216.1	0.01	266	117	0.45	87.8	2,099	±18	2,051	±7.7	-2	0.1266	0.44	6.718	1.1	0.3848	1	0.919
217.1	0.35	180	89	0.51	52.3	1,875	±17	2,037	±12	8	0.12559	0.7	5.845	1.2	0.3376	1	0.829
218.1	–	116	48	0.43	36.6	2,019	±19	2,067	±11	2	0.12776	0.62	6.479	1.3	0.3678	1.1	0.871
219.1	0.04	192	79	0.42	61.5	2,039	±18	2,043	±9.8	0	0.12606	0.55	6.467	1.2	0.372	1	0.881
220.1	0.08	161	78	0.5	51.2	2,024	±18	2,061	±14	2	0.12733	0.77	6.475	1.3	0.3688	1.1	0.80
221.1	0.11	159	68	0.44	51	2,045	±19	2,048	±10	0	0.12636	0.57	6.504	1.2	0.3733	1.1	0.885
222.1	–	228	86	0.39	72.4	2,032	±18	2,075	±8.3	2	0.12837	0.47	6.559	1.1	0.3706	1	0.908
223.1	0.01	124	52	0.43	40.3	2,061	±19	2,029	±11	-2	0.12505	0.63	6.495	1.3	0.3767	1.1	0.866
224.1	3.54	599	680	1.17	133	1,426	±13	2,120	±42	33	0.1317	2.4	4.49	2.6	0.2476	1	0.385
225.1	0.06	130	52	0.42	42.1	2,064	±19	2,055	±15	0	0.1268	0.83	6.601	1.4	0.3774	1.1	0.801
226.1	0.09	196	91	0.48	62.8	2,040	±19	2,050	±9.2	1	0.12657	0.52	6.497	1.2	0.3723	1.1	0.897
227.1	0.1	127	54	0.44	41.4	2,070	±19	2,053	±11	-1	0.12671	0.65	6.615	1.3	0.3786	1.1	0.859
228.1	0.14	174	77	0.46	56.4	2,066	±18	2,044	±9.7	-1	0.12613	0.55	6.569	1.2	0.3777	1	0.885
229.1	0.08	173	78	0.47	55.6	2,045	±18	2,047	±10	0	0.12633	0.59	6.502	1.2	0.3733	1	0.872
230.1	0.23	92	40	0.45	28.8	2,008	±22	2,045	±20	2	0.1262	1.1	6.36	1.7	0.3654	1.3	0.744
231.1	0.05	104	47	0.46	33.7	2,065	±20	2,070	±13	0	0.12799	0.73	6.662	1.4	0.3775	1.2	0.847
232.1	–	152	63	0.43	48.5	2,042	±19	2,075	±10.0	2	0.12838	0.57	6.598	1.2	0.3728	1.1	0.882
11A.1	0	249	108	0.45	80.5	2,057	±18	2,074	±7.7	1	0.12824	0.43	6.646	1.1	0.3759	1	0.917
12.1	–	164	68	0.43	52.9	2,058	±18	2,058	±9.3	0	0.12708	0.53	6.592	1.2	0.3762	1	0.892
13.1	0	176	70	0.41	56.9	2,061	±18	2,072	±9.2	1	0.12812	0.52	6.655	1.2	0.3767	1	0.895
14.1	–	138	70	0.52	45.1	2,075	±19	2,068	±10	0	0.12779	0.59	6.69	1.2	0.3797	1.1	0.876
15.1	–	254	138	0.56	81	2,037	±18	2,055	±8.5	1	0.12689	0.48	6.501	1.1	0.3716	1	0.903
16.1	–	198	87	0.46	64.8	2,081	±18	2,059	±8.6	-1	0.12715	0.49	6.681	1.1	0.3811	1	0.903
17.1	9.57	1574	1030	0.68	148	596	±22	2,060	±140	71	0.1273	7.7	1.7	8.8	0.0968	3.8	0.431
18.1	0.13	157	65	0.43	50.9	2,063	±19	2,049	±11	-1	0.12644	0.61	6.575	1.2	0.3771	1.1	0.865
19.1	0.64	243	157	0.67	73.4	1,926	±17	2,045	±13	6	0.12616	0.73	6.057	1.2	0.3482	1	0.807
110.1	11.89	988	255	0.27	160	968	±18	1,843	±250	47	0.113	14	2.52	14	0.162	2.3	0.164

Errors are 1-sigma; Pb_c and Pb^* indicate the common and radiogenic portions, respectively. Error in Standard calibration was 0.28% (not included in above errors but required when comparing data from different mounts). (1) Common Pb corrected using measured ^{204}Pb.

(Figure 3). If the correlation of the Loskop and Glentig Formations with WUBS I is accepted (Figure 3), our results also imply that these successions postdate rather than predate, as previously thought (Cheney and Twist, 1986), the intrusion of the mafic-ultramafic phase of the Bushveld Complex (Figure 9).

Regardless of whether the correlation with the Loskop Formation is accepted or not, the paraconformable nature of the contact between the pre-Bushveld Rooiberg felsites and the post-Bushveld Lower Swaershoek Formation (WUBS I) indicates that the felsite beds were not tilted or deformed during intrusion of the Bushveld Complex. The limited area occupied by WUBS I relative to the overall size of the Bushveld Complex makes it impossible to ascertain how widely this feature applies, but it is certainly valid for the Central Bushveld domain around Nylstroom and Rust de Winter between the western and eastern limbs of the Bushveld Complex (Figure 1). This mild deformation in the roof of the Bushveld is in contrast to the intensive folding and deformation that *e.g.* Transvaal strata experienced in the floor of the Bushveld Complex immediately to the east and west of the central domain in the Marble Hall and Crocodile River inliers (Hartzer, 2000). A simple explanation for these observations would be that at shallow depth space for the intrusion of the Bushveld Complex was made by mere uplift of the roof rocks of the magma chamber, releasing stress and causing little lateral deformation of roof rocks. At depth, in the floor of the complex, the opposite applied, and the creation of space for the magma intrusion must have involved considerable lateral shortening of the wall rocks.

Because of the paraconformable nature of the contact between the Rooiberg felsite and the Lower Swaershoek Formation (WUBS I), it is concluded that not much erosion of Rooiberg strata took place prior to deposition of the basal Waterberg beds. The thickness of the Rooiberg strata preserved below the Waterberg Group should thus approximate the depth of intrusion of the Bushveld Complex, especially the granitic phase. The thickness of the Rooiberg strata is consistently in the order of 3 to 4.5 km according to data provided in an overview of the Rooiberg Group by Schweitzer *et al.* (1995).

Tilting and faulting of strata in the roof of the Bushveld Complex appear to have become more pronounced only after deposition of WUBS I. Contemporaneous faulting during deposition of WUBS I is only locally pronounced in parts of the Loskop Formation, which contains excellent examples of fault scarp-derived deposits (Martini, 1998). Tilting of strata after deposition of WUBS I is indicated by the fact that the overlying unconformity-bounded sequence (WUBS II) unroofs granite of the Bushveld Complex and overlies strata of the Loskop Formation with marked angular unconformity near Middelburg (Jansen, 1982) (Figure 3A). Near Nylstroom, faulting of WUBS I also took place prior to deposition of WUBS II (Cheney and Twist, 1986). These structural and stratigraphic relations are perhaps best explained by thermal adjustments in the crust during the waning stages of, and immediately following the intrusion of the Bushveld Complex (Figure 9).

Paleomagnetic data from the Waterberg Group (de Kock *et al.,* 2006) show a large shift in Kaapvaal apparent pole positions between WUBS I and WUBS II (Figure 9). A grand mean of paleomagnetic results from the Main and Upper Zones of the Bushveld Complex (Evans *et al.*, 2002) occupies and intermediate position between the two lower Waterberg poles, and the Bushveld remanence was acquired prior to the gentle synclinal folding of the eastern and western limbs of the complex. Thus it appears that such folding occurred between deposition of WUBS I and WUBS II.

After deposition of WUBS II (Upper Swaershoek and Alma Formations), folding of strata took place to form the main phase of deformation in the Nylstroom syncline. The result is that WUBS III rests with a marked angular unconformity on WUBS II in the Nylstroom area (Figure 3A). This fold event relates to intermittent reactivation of the Thabazimbi-Murchison Lineament (Figure 1).

Age relations between the Waterberg and Soutpansberg Groups

Our new concordant age of 2021 ± 5 Ma for the Entabeni Granite provides a reliable lower limit for deposition of the nonconformably overlying Soutpansberg Group. However, there may be a considerable hiatus between intrusion and subsequent unroofing of the granite and the deposition of the Soutpansberg Group (Figure 9). Hydrothermally altered lava flows and sills from the Sibasa Formation in the lower part of the Soutpansberg Group previously yielded poorly constrained Rb-Sr ages of 1749 ± 104 Ma and 1769 ± 34 Ma (Barton, 1979) and a Pb-Pb whole rock age of 1809 + 263/-317 for the same lava samples (Cheney *et al.*, 1990). These imprecise ages are interpreted to reflect hydrothermal alteration of the lavas after deposition, and therefore only provide a lower age limit for the extrusion of the volcanic rocks of the Soutpansberg Group (Figure 9).

The Soutpansberg Group also nonconformably overlies mylonites of the Palala Shear Zone (Figure 1). Syntectonic biotite from this shear zone yielded a Rb-Sr age of 1971 ± 26 Ma (Schaller et al., 1999) and probably provides a closer estimate to onset of deposition of the Soutpansberg Group than our concordant age of 2021 ± 5 Ma on the Entabeni Granite. A Rb-Sr age of 1974 ± 14 Ma on muscovite (Cheney *et al.*, 1990) and the discordant U-Pb zircon age of 1957 ± 3 Ma on the same sample set of the Entabeni Granite (Barton *et al.*, 1995) are within error of the Rb-Sr age of biotite from the Palala Shear Zone, and probably reflect a subtle overprint of this major event of shearing on the Entabeni Granite.

From the above reasoning it follows that the Sibasa lavas must have formed between ~1.76 Ga, the timing of

Table 2. Summary of SHRIMP U-Pb data for zircons from the quartz porphyry lava of the Rust de Winter Formation.

Grain.Spot	(1) % $^{206}Pb_c$	ppm U	ppm Th	$^{232}Th/^{238}U$	ppm $^{206}Pb^*$	(1) $^{206}Pb/^{238}U$ Age		(1) $^{207}Pb/^{206}Pb$ Age		% Discordant	Total $^{238}U/^{206}Pb$	±%	Total $^{207}Pb/^{206}Pb$	±%	(1) $^{238}U/^{206}Pb^*$	±%	(1) $^{207}Pb^*/^{206}Pb^*$	±%	(1) $^{207}Pb^*/^{235}U$	±%	(1) $^{206}Pb^*/^{238}U$	±%	errcorr
1.1	0.34	156	67	0.44	50.7	2,059	±21	2,033	±21	-1	2.649	1.2	0.1283	0.85	2.658	1.2	0.1253	1.2	6.5	1.7	0.3762	1.2	0.715
2.1	0.77	863	331	0.4	249	1,856	±12	1,983	±16	6	2.974	0.76	0.12855	0.49	2.997	0.77	0.1218	0.92	5.605	1.2	0.3337	0.77	0.642
3.1	0.61	348	205	0.61	105	1,928	±15	2,059	±16	6	2.851	0.92	0.13255	0.58	2.869	0.93	0.1271	0.88	6.111	1.3	0.3486	0.93	0.723
4.1	1.07	882	449	0.53	246	1,797	±14	1,957	±14	8	3.076	0.91	0.1295	0.43	3.11	0.92	0.12008	0.77	5.324	1.2	0.3216	0.92	0.765
5.1	0	411	199	0.5	133	2,060	±16	2,052	±9.2	0	2.655	0.88	0.12671	0.52	2.655	0.88	0.12671	0.52	6.579	1	0.3766	0.88	0.86
6.1	2.95	521	286	0.57	134	1,639	±12	2,029	±26	19	3.352	0.84	0.151	0.49	3.454	0.86	0.125	1.5	4.99	1.7	0.2895	0.86	0.508
7.1	2.03	1177	523	0.46	190	1,088	±7.5	1,708	±22	36	5.325	0.74	0.12227	0.43	5.435	0.75	0.1046	1.2	2.654	1.4	0.184	0.75	0.536
8.1	1.93	1899	410	0.22	139	517.3	±3.6	1,750	±25	70	11.738	0.72	0.12385	0.71	11.969	0.73	0.1071	1.4	1.233	1.6	0.08355	0.73	0.47
9.1	0.32	351	180	0.53	108	1,961	±16	2,057	±16	5	2.803	0.92	0.12981	0.63	2.812	0.92	0.127	0.92	6.227	1.3	0.3556	0.92	0.71
10.1	0.03	395	277	0.72	129	2,083	±16	2,040	±9.7	-2	2.62	0.89	0.12613	0.54	2.621	0.89	0.12585	0.55	6.62	1	0.3815	0.89	0.852
11.1	0.07	596	331	0.57	191	2,043	±14	2,054	±8.2	1	2.68	0.81	0.12737	0.44	2.682	0.81	0.12679	0.46	6.519	0.93	0.3729	0.81	0.868
12.1	0.59	1337	743	0.57	129	682.8	±5.0	1,898	±15	64	8.898	0.76	0.12135	0.53	8.951	0.77	0.11619	0.86	1.79	1.2	0.11172	0.77	0.668
13.1	11.36	2171	3256	1.55	175	514.7	±4.8	1,438	±85	64	10.665	0.84	0.18792	0.38	12.03	0.96	0.0906	4.4	1.038	4.5	0.08311	0.96	0.211
14.1	10.21	1346	1391	1.07	159	749.4	±5.8	1,558	±60	52	7.284	0.74	0.18451	0.41	8.112	0.82	0.0965	3.2	1.641	3.3	0.1233	0.82	0.248
15.1	0.16	208	99	0.49	68.1	2,076	±19	2,051	±15	-1	2.628	1.1	0.12799	0.74	2.632	1.1	0.1266	0.86	6.631	1.4	0.38	1.1	0.781
16.1	0.61	456	228	0.52	146	2,036	±15	2,054	±13	1	2.677	0.87	0.13218	0.51	2.693	0.87	0.1268	0.76	6.492	1.2	0.3713	0.87	0.752
17.1	0.32	302	162	0.55	88.7	1,891	±16	2,054	±15	8	2.924	0.95	0.12963	0.63	2.934	0.95	0.1268	0.85	5.96	1.3	0.3409	0.95	0.748

Errors are 1-sigma; Pb_c and Pb^* indicate the common and radiogenic portions, respectively. Error in Standard calibration was 0.33% (not included in above errors but required when comparing data from different mounts). (1) Common Pb corrected using measured ^{204}Pb.

hydrothermal alteration, and ~1.97 Ga, the final phase of ductile deformation along the Palala Shear Zone. However, there is indirect evidence from the Blouberg area (Figure 1) that the Sibasa lavas extruded at ~1.87 Ga or somewhat later. This evidence comes from a dolerite dyke swarm that intrudes the Mogalakwena Formation (part of WUSB V) of the Waterberg Group immediately south of the Melinda fault zone (Figure 3A), and correlative rocks to the north of the fault zone (Bumby *et al.*, 2001). These dykes, which are similar in composition to the Sibasa lavas of SUBS I (Bumby *et al.*, 2001) do not cut the quartzites of the Wyllies Poort Formation of the upper unconformity-bounded sequence SUBS II (Figure 4). Bumby *et al.* (2001), therefore, suggested that these dykes acted as feeders for the Sibasa lavas. Unfortunately these dykes have not been directly dated. On geological maps, they appear to cross cut the dolerite sills that also intrude the Mogalakwena Formation and for which Hanson *et al.* (2004) reported U-Pb baddeleyite ages of ~1.88 to ~1.87 Ga. The dolerite dyke swarm may thus either represent a late phase of the sills or they could be younger. That implies that the Sibasa lavas flowed out at ~ 1.88 Ga or somewhat later, between ~1.88 Ga and ~1.76 Ga (Figure 9).

The sills intruding the Mogalakwena Formation provide a minimum age constraint of ~1,875 Ga (Hanson *et al.*, 2004) for nearly the entire Waterberg Group, at least up to the lower part of WUBS V (Figure 9). Most of the Waterberg Group, therefore, pre-dates deposition of the Soutpansberg Group. There is, however, uncertainty about the age of the uppermost Cleremont and Vaalwater Formations of the Waterberg Group, because they are not intruded by the ~1.88 Ga sills (Hanson *et al.*, 2004).

Apart from the age of the Sibasa lava, there is also the question of the age of the Nzhelele lavas in the upper unconformity-bounded sequence (SUBS II) of the Soutpansberg Group. Paleomagnetic studies by Hanson *et al.* (2004) on one site of Sibasa lava, one on Nzhelele lava and five on dolerite sills that intrude both the Sibasa and Wyllies Poort Formations, i.e. SUBS I and II (Figure 4), in the Soutpansberg Mountain Range, yielded a tight site mean direction which is antipodal at 95% confidence level to a site mean obtained from six sites of the ~1.88 Ga dolerite sills that intrude WUBS II of the Waterberg Group (Figure 9). Based on this data, Hanson *et al.* (2004) suggested that intrusion of the ~1.88 Ga dolerite sills in the Waterberg Group coincided with extrusion of the Sibasa lavas of the Soutpansberg Group. However, the sills sampled by Hanson *et al.* (2004) in the Soutpansberg Mountains intrude both the lower (SUBS I) and upper (SUBS II) unconformity-bounded sequences of the Soutpansberg Group and must, therefore, post-date the pre-Wyllies Poort dolerite dyke swarm described by Bumby *et al.* (2001) from the Blouberg area. This implies that there is a younger, post-Wyllies Poort, suite of dolerite sills intruded into

Table 3. Summary of SHRIMP U-Pb data for zircons from the Entabeni Granite

Spot	(1)	ppm	ppm		ppm	(1)		(1)		%	(l)	±%	(l)	±%	(1)	±%	errcorr
	%	U	Th	$^{232}Th/^{238}U$	$^{206}Pb^*$	$^{206}Pb/^{238}U$		$^{207}Pb/^{206}Pb$		Discordant	$^{207}Pb^*/^{206}Pb^*$		$^{207}Pb^*/^{235}U$		$^{206}Pb^*/^{238}U$		
	$^{206}Pb_c$					Age		Age									
1.1	0.09	214	105	0.51	66.6	1,992	±20	2,008	±8.2	1	0.12356	0.46	6.17	1.3	0.3621	1.2	0.931
1.2	0.09	244	125	0.53	77.7	2,030	±23	2,004	±9.0	-1	0.12328	0.51	6.29	1.4	0.37	1.3	0.935
2.1	0.06	237	113	0.49	75.3	2,030	±23	2,024	±7.2	0	0.1247	0.41	6.363	1.4	0.37	1.3	0.956
3.1	10.01	3091	1029	0.34	271	565.7	± 3.2	1,605	±50	65	0.099	2.7	1.252	2.7	0.09172	0.59	0.215
4.1	0.05	226	125	0.57	70.8	2,001	±13	2,020	±7.5	1	0.12438	0.42	6.241	0.87	0.3639	0.76	0.873
5.1	8.38	809	580	0.74	241	1,776	±11	2,070	±86	14	0.128	4.9	5.6	4.9	0.3171	0.74	0.15
6.1	0.61	441	342	0.8	130	1,888	±12	2,015	±9.3	6	0.12406	0.53	5.822	0.92	0.3404	0.75	0.82
7.1	0.1	382	247	0.67	116	1,953	±13	2,019	±7.0	3	0.12436	0.39	6.068	0.89	0.3539	0.79	0.897
8.1	3.45	325	176	0.56	109	2,063	±25	2,065	±44	0	0.1276	2.5	6.63	2.9	0.3771	1.4	0.492
9.1	0.01	335	205	0.63	104	1,987	±12	2,031	±6.7	2	0.12521	0.38	6.234	0.78	0.3611	0.69	0.874
10.1	0.03	256	170	0.69	79.6	1,991	±12	2,029	±8.1	2	0.12503	0.46	6.239	0.83	0.3619	0.7	0.835
11.1	0.71	341	300	0.91	101	1,902	±11	2,015	±11	6	0.12401	0.61	5.868	0.91	0.3432	0.68	0.74
12.1	0.16	394	254	0.67	125	2,021	±13	2,028	±7.9	0	0.12496	0.44	6.345	0.85	0.3682	0.72	0.853
13.1	0.06	225	121	0.56	69	1,965	±15	2,008	±9.0	2	0.12358	0.51	6.072	1	0.3564	0.9	0.869
14.1	0.04	243	138	0.59	75.5	1,986	±19	2,017	±8.4	2	0.12419	0.47	6.177	1.2	0.3607	1.1	0.919
15.1	0.2	378	223	0.61	120	2,021	±16	2,008	±9.5	-1	0.12355	0.54	6.273	1.1	0.3683	0.91	0.861
15.2	0.17	290	163	0.58	92	2,021	±21	2,005	±8.4	-1	0.12336	0.47	6.264	1.3	0.3682	1.2	0.932
16.1	5.25	932	607	0.67	300	1,959	±11	1,989	±40	2	0.1222	2.2	5.98	2.3	0.3551	0.67	0.29

Errors are 1-sigma; Pb_c and Pb^* indicate the common and radiogenic portions, respectively. Error in Standard calibration was 0.61% (not included in above errors but required when comparing data from different mounts). (1) Common Pb corrected using measured ^{204}Pb.

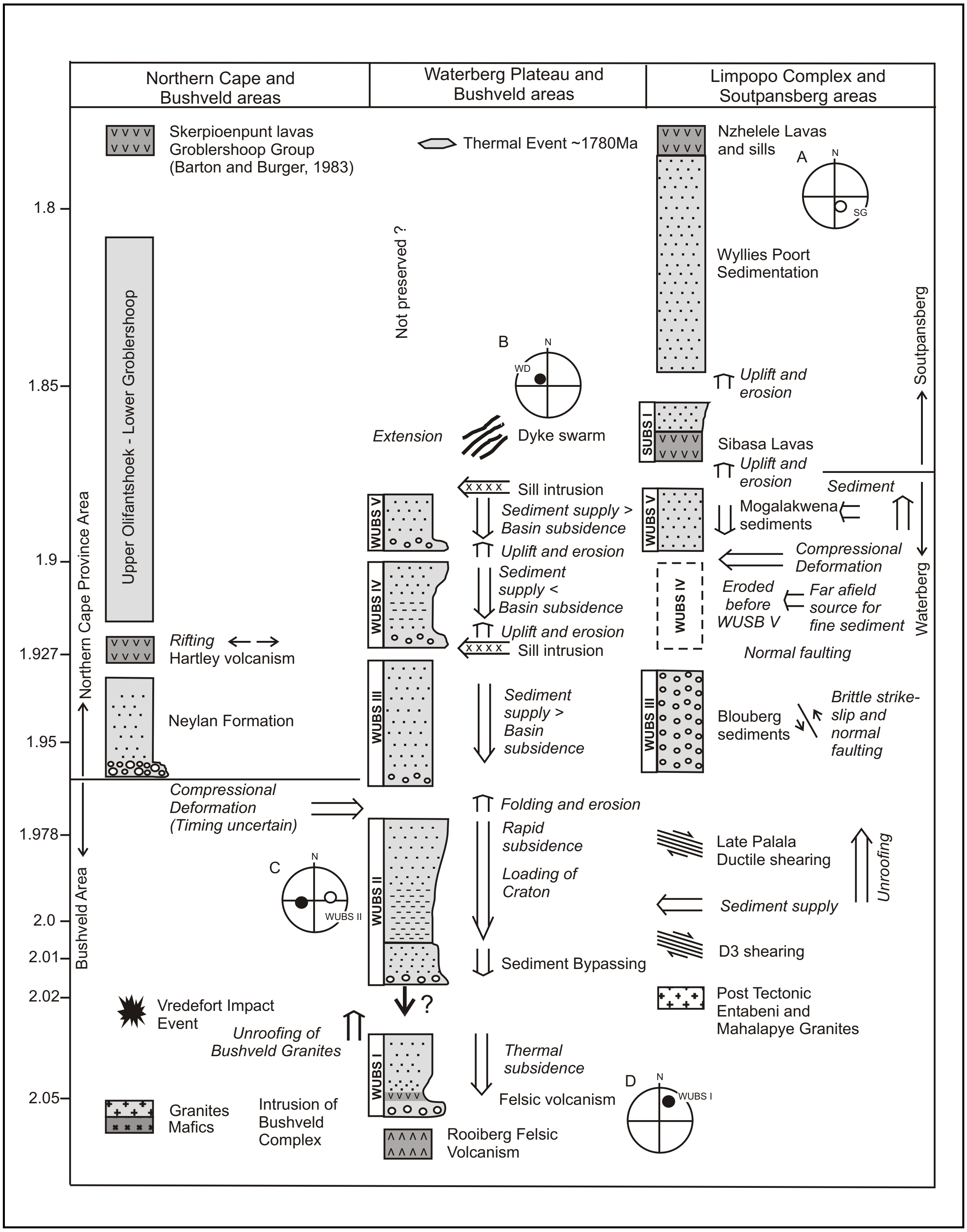

Figure 9. Schematic presentation of the geological and chronostratigraphic development of the Waterberg and Soutpansberg successions and their relation to magmatic and tectonic events associated with the Bushveld Complex and Limpopo Metamorphic Complex. The insets of stereographic plots show the paleomagnetic directions obtained by Hanson *et al.* (2004) on ~1875 Ma sills of the Waterberg Group (**B**) and the combined direction (lower hemisphere SG) for Sibasa and Nzhelele lava and sills intruding the Wyllies Poort Formation. (**A**) and by de Kock *et al.* (2006) on WUBS II (**C**) and I (**D**). Note the shift in paleomagnetic directions from WUBS I to WUBS II (stereographic plot B). Also note synchroneity of Vredefort structure with intrusion of anorogenic granites in the Limpopo Complex at ~2.02 Ga. References relevant to the compilation of the diagram are given in the text.

Soutpansberg Group rocks for which we have as yet no direct isotopic age (Figure 9). The paleomagnetic pole obtained by Hanson *et al.* (2004) on these younger sills must therefore post-date that obtained by the same authors on the ~1.87 Ga sills intruded into the Waterberg Group. The pole on the younger post-Wyllies Poort sills, therefore, most probably represents a magnetic reversal rather than an antipole to the ~1.87 Ga pole (Figure 9).

It is possible that the Nzhelele lavas and post-SUBS II sills represent a thermal event that caused the resetting of Rb-Sr and Pb-Pb isotopic systems at ~1.76 Ga, documented by Barton (1979) and Cheney *et al.* (1990), in Sibasa lavas (Figure 9). This younger ~1.76 Ga igneous event may have been very widespread because the Skerpioenpunt lavas in the Groblershoop Group, overlying the Olifantshoek Group (Figure 1), have a similar Ar/Ar age (Barton and Burger, 1983) (Figure 9).

Waterberg Sedimentation and Limpopo Tectonism

The concordant zircon age of 2021 ± 5 Ma obtained on the Entabeni Granite in the Southern Marginal Zone of the Limpopo Complex is virtually identical to the 2024 ± 7 Ma U-Pb SHRIMP zircon age of the very prominent post-tectonic Mahalapye Granite (Figure 1) in the Central Zone of the Complex (Gutzmer and Beukes, 1998; McCourt and Armstrong, 1998). The ages of these post-tectonic (McCourt and Armstrong, 1998) or anorogenic (Barton *et al.*, 1995) granites are also in virtual exact correspondence to the timing of the thermal peak of metamorphism in the Central Zone of the Limpopo Complex, dated with zircon at 2027 ± 6 Ma (Jaeckel *et al.*, 1997, Barton *et al.*, 2006). This would imply that the widespread ~2.02 to ~2.03 Ga metamorphic event in the Central Zone of the Limpopo Complex (*e.g.* Holzer *et al.*, 1998; 1999; Hisada and Miyano, 1996) is of thermal rather than collisional origin as previously considered (*e.g.* Barton *et al.*, 1994; 2006; Kröner *et al.*, 1999). Metamorphic mineral ages recorded in the Limpopo Complex that are younger than the post-tectonic ~2.02 Ga Entabeni and Mahalapye granites, are typically associated with late shear zones which record a period of non-penetrative deformation in the complex. These mineral ages fall in two age groups, namely around ~2.01 Ga dating the D3 shear event in the Limpopo Complex (McCourt and Armstrong, 1998) and at ~1.97 Ga recording the latest deformation in, for example, the Palala Shear Zone (Schaller *et al.*, 1999). The origin of the ~2.03 Ga thermal activity and later non-penetrative shear deformation in the Central Zone of the Limpopo Complex is uncertain, but it may be related to orogenesis in the to ~2.03 to ~1.95 Ga (Mapeo *et al.*, 2001) Magondi belt along the western margin of the Zimbabwe Craton.

The four lower unconformity-bounded sequences of the Waterberg Group (WUBS I-IV) are confined to the Kaapvaal Craton south of the Palala Shear Zone whereas the upper sequence (WUBS V) discordantly transgresses the shear zone (Figure 3A). Our new age of 2054 Ma for the base of the Waterberg Group indicates that WUBS I-IV were most likely deposited coeval with the 2.0 ± 0.05 Ga magmatic and tectonic events in the Limpopo Complex, in contrast to WUBS V that postdates the latter events. That there is almost certainly a relationship between deposition of the Waterberg Group and tectonic events in the Limpopo Complex is indicated by the fact that virtually all of the siliciclastic sedimentary rock units of the Waterberg Group coarsen in direction of the Limpopo Complex (Cheney and Twist, 1986).

The exact relations between deposition of WUBS I-IV and the 2.0 ± 0.05 Ga magmatic and tectonic events in the Limpopo Complex remain uncertain. However, there is sufficient age and geological data available to support the following scenario. As discussed earlier, indications are that deposition of WUBS I took place during and immediately after intrusion of the granitic phase of the Bushveld Complex (Figure 9). Basin subsidence at that time may have been largely controlled by late syn- to early post-Bushveld thermal uplift and subsidence. However, by the time of deposition of WUBS II, granites of the Bushveld Complex were unroofed and cooled down such that uplift and subsidence of the Waterberg basin were controlled by external tectonic or thermal magmatic events independent of Bushveld magmatism. The most likely external candidates are the 2.0±0.05 Ga thermal and tectonic events in the Limpopo Complex. Early phases of these events, including intrusion of the Entabeni and Mahalapye granites at 2025 Ma, may have affected deposition of the Waterberg Group. The lower part of WUBS II, represented by the Upper Swaershoek Formation, is a very coarse sandy to boulder conglomerate fluvial succession indicating active tectonic uplift in source areas coupled with a sediment supply rate which overwhelmed basin subsidence rate so that bypassing of most fine sediment took place. It is interesting to note that the ages of the Entabeni and Mahalapye granites correspond almost exactly with the 2023 ± 4 Ma age of the Vredefort meteorite impact structure (Kamo *et al.*, 1996). Another important observation is that the spatial ordering of paleomagnetic poles from WUBS I (de Kock *et al.*, 2006), to Bushveld complex (reviewed by Evans *et al.*, 2002), to the Vredefort structure (reviewed by Evans *et al.*, 2002), to WUBS II (de Kock *et al.*, 2006) suggests that the middle to upper parts of WUBS II are younger than ca. 2020 Ma. Thus, if onset of deposition of WUBS II indeed coincided with intrusion of the granites at ~2023 Ma the search for ejecta from the Vredefort impact should focus along the base of WUBS II.

The Upper Swaershoek Formation in the lower part of WUBS II is overlain by shale and fine graywackes of the Alma Formation, which is up to 3000 m thick (Figure 2). This implies a period of very rapid subsidence rate in the basin with creation of sufficient accommodation space to trap fine siliciclastics. It is conceivable that this stage of development of the Waterberg basin relates to the ~2.01 to ~1.97 Ga interval of non-penetrative shearing and thrusting in the Limpopo Complex (Figure 9). The Palala shear zone is essentially strike-slip (McCourt and Armstrong, 1998; Schaller *et al.*, 1999), but some of the shears tangentially merging with it to the north in the Central Zone of the Limpopo Complex have a southwesterly merging thrust component (Carney *et al.*, 1994), so that subsidence of the Waterberg basin at that time could have been the result of both strike-slip deformation and thrust loading. This would place deposition of WUBS II in the interval ~2.02 to ~1.97 Ga (Figure 9).

Deposition of WUBS II came to an end following uplift and erosion related to a period of north-south directed crustal shortening and folding specifically well developed near the Thabazimbi-Murchison Lineament. Along this lineament folding of WUBS I and II took place prior to deposition of WUBS III (Figures 1 and 3A). The cause of this crustal shortening event, which not only reactivated the Thabazimbi-Murchison Lineament but also affected other strata on the Kaapvaal Craton as far south as the Witwatersrand area (Van Niekerk *et al.*, 1999) is unknown. Either it is manifestation of a north-directed, compressional orogen that was situated to the south of the Kaapvaal Craton at that time, and that has since rifted away, or it represents far-field deformation related to the Limpopo Complex towards the end of deposition of WUBS II.

Undeformed strata of WUBS III and IV extend northwards to the southern margin of the Palala Shear Zone but do not cross the margin. The first beds of the Waterberg Group that overlie the Palala Shear Zone are the virtually flat-lying and undeformed strata of the Mogalakwena Formation in the lower part of WUBS V (Figure 3A). This formation is intruded by ~1.88 Ga dolerite sills (Hanson *et al.*, 2004) which implies that it is older than ~1.87 Ga but younger than ~1.97 Ga, the time of ductile deformation in the Palala Shear Zone (Figure 9). However, it is important to note that the undeformed beds of the Mogalakwena Formation overlie steeply dipping folded and thrusted coarse red beds of the Blouberg Formation with a marked angular unconformity near the Palala Shear Zone (Bumby *et al.*, 2001). These deformed red beds of the Blouberg Formation non-conformably overlie ductile mylonites in the Palala Shear Zone which means that they were deposited after ~1.97 Ga but before shallow brittle deformation came to end in the shear zone. The very coarse and immature nature of the Blouberg red beds make them unlikely correlatives of the aeolian quartzite of the Makgabeng Formation of WUBS IV(Figure 3B). However, there is no reason why the Blouberg beds could not be lateral equivalents of the Setlaole Formation (WUBS III) that were deposited in very proximal environments in pull-apart basins associated with late brittle deformation along the Palala Shear Zone (Bumby *et al.*, 2001). In Botswana near Kanye, strata of the Mannyelanong Formation of the Waterberg Group are intruded by 1927 ± 0.7 dolerite sills (Hanson *et al.*, 2004) (Figure 1). If the correlation of the Mannyelanong Formation with the Skilpadkop and Setlaole Formations is correct (Figure 3B), then it means that WUBS III was deposited before ~1.93 Ga and after ~1.97 Ga (Figure 9). Unfortunately we have no direct information available up to which stratigraphic level in the Waterberg Group the ~1.93 Ga dolerites may have intruded (Hanson *et al.*, 2004).

In the Blouberg area, it is clear that deposition of the Blouberg Formation was followed by a distinct south-verging compressional event which folded and thrusted both the schistose mylonitic fabric of the Palala Shear Zone and red beds of the Blouberg Formation (Bumby *et al.*, 2001). It is this interval of deformation that preceded deposition of the very coarse red beds of WUBS V. In contrast, sedimentary rocks of WUBS IV are fine grained and must have been derived from a distal source when the Palala Shear Zone was inactive (Figure 9).

The ~1.93 Ga sills that intrude the Mannyelanong Formation near Kanye, are similar in age to the Hartley lavas (Cornell *et al.*, 1998) of the Olifantshoek Group along the western margin of the Kaapvaal Craton in Griqualand West (Figure 1). These lavas are underlain by the basal Neylan Conglomerate Formation and overlain by the Volop Formation of the Olifantshoek Group (Dorland, 2004). If the correlation of the Mannyelanong Formation with WUBS III is accepted (Figure 3B), it implies that the Neylan Formation could be time-equivalent to at least WUBS I-III. If we further assume that the ~1.93 Ga sills intruded prior to deposition of WUBS IV, for which we unfortunately have no concrete evidence as noted earlier, then it would imply that the upper two unconformity-bounded sequences of the Waterberg Group (WUBS IV and V) could correlate in time with the Volop Formation (Figure 9). The Palapye Group, which erosively overlies the ~2.02 Ga Mahalapye Granite in Botswana (Figure 1), could in part be time-equivalent to the Waterberg and Soutpansberg Groups (Mapeo *et al.*, 2004; Dorland, 2004). However, the uppermost Lotsane Formation of the Palapye Group, which contains 1604 ± 33 Ma old zircons (Mapeo *et al.*, 2004), most probably post-dates even the upper Nzhelele Formation of the Soutpansberg Group for which we suggest an age of ~1.78 Ga (Figure 9).

Conclusion

A precise SHRIMP U-Pb zircon age of 2054 ± 4 Ma obtained on quartz porphyry lava near the base of the Lower Swaershoek Formation of the Waterberg Group indicates that deposition of this succession was contemporaneous with, or followed shortly after, intrusion of the granitic phase of the Bushveld Complex. The porphyritic lavas form part of the basal unconformity-bounded sequence of the Waterberg Group (WUBS I), which is correlative with the Rust de Winter, Glentig and Loskop Formations. These successions were previously considered to be older than the Bushveld Complex, but our age data now indicate that they are younger.

A precise SHRIMP U-Pb zircon age of 2021 ± 5 Ma on the Entabeni Granite, provides a reliable maximum age for the Soutpansberg Group, which overlies the granite with an erosional contact. There is, however, indirect evidence that the Sibasa lavas, near the base of the Soutpansberg Group are ≤ 1875 Ma which implies a hiatus of at least 150 Myr between intrusion of the Entabeni Granite and deposition of the Soutpansberg Group.

Dolerite sills that intrude the upper Formations of the Waterberg Group were dated by Hanson *et al*. (2004) at ~1875 Ma. Most of the Waterberg Group, therefore, must have been deposited in the period ~2054 to ~1875 Ma, which makes it older than the Soutpansberg Group (Bumby *et al.*, 2001; Hanson *et al.*, 2004) but places it within the time frame of the 2000 ± 50 Ma thermal metamorphic and non-penetrative shear deformation events in the Limpopo Metamorphic Complex. Deposition of the Waterberg Group and development of the basin could thus be coupled to tectono-metamorphic events in the Limpopo Complex.

Acknowledgements

Research of Dorland, Beukes and Gutzmer were funded by a grant from the National Research Foundation to NJB, that of Evans by grants from the Australian Research Council and Agouron Institute, and of Armstrong by PRISE at ANU in Canberra. Constructive reviews by A. Bumby and G. Brandl are gratefully acknowledged.

References

Barker, O.B. (1983). A proposed geotectonic model for the Soutpansberg Group within the Limpopo Mobile Belt, South Africa. *Special Publication of the Geological Society of South Africa*, **8**, 181-190.

Barton, E.S. and Burger, A.J. (1983). Reconnaissance isotopic investigations in the Namaqua mobile belt and implications for Proterozoic crustal evolution -- Upington geotraverse. *Special Publication of the Geological Society of South Africa*, **10**, 173-192.

Barton, J.M. (1979). The chemical compositions, Rb-Sr isotopic systematics and tectonic setting of certain post-kinematic mafic igneous rocks, Limpopo Mobile Belt, southern Africa. *Precambrian Research*, **9**, 57-80.

Barton, J.M., Doig, R. and Smith, C.B. (1995). Age, origin, and tectonic significance of the Entabeni granite, northern Transvaal, South Africa. *South African Journal of Geology*, **98**, 326-330.

Barton, J.M. Jr., Holzer, L., Kamber, B., Doig, R., Kramers, J.D. and Nyfeler, D. (1994). Discrete metamorphic events in the Limpopo belt, southern Africa: implications for the application of P-T paths in complex metamorphic terranes. *Geology*, **22**, 1035-1038.

Barton, J.M. Jr., Klemd, R. and Zeh, A. (2006). The Limpopo Belt: A Result of Archean to Proterozoic, Turkic-Type Orogenesis? *In:* W.U. Reimold and R.L. Gibson (Editors), Processes on the early Earth. *Geological Society of America, Special Paper,* **405**, 315-332.

Buick, I.S., Maas, R. and Gibson, R. (2001). Precise U-Pb titanite age constraints on the emplacement of the Bushveld Complex, South Africa. *Journal of the Royal Geological Society, London*, **158**, 3-6.

Bumby, A.J., Eriksson, P.G., Van Der Merwe, R. and Maier, W.D. (2001). The stratigraphic relationship between the Waterberg Group and the Soutpansberg Group (Northern Province, South Africa): Evidence from the Blouberg area. *South African Journal of Geology,* **104**, 205-216.

Callaghan, C.C., Eriksson, P.G. and Snyman, C.P. (1991). The sedimentology of the Waterberg Group in the Transvaal, South Africa: an overview. *Journal of African Earth Sciences*, **13**, 121-139.

Carney, J.N., Aldiss, D.T. and Lock, N.P. (1994). The Geology of Botswana. *Bulletin of the Geological Survey of Botswana*, **37**, 113 pp.

Cheney, E.S. and Twist, D. (1986). The Waterberg "Basin" – A reappraisal. *Transactions of the Geological Society of South Africa*, **89**, 353-360.

Cheney, E.S., Barton, J.M. and Brandl, G. (1990). Extent and age of the Soutpansberg sequences of southern Africa. S*outh African Journal of Geology*, **93**, 664-675.

Coertze, F.J., Jansen, H. and Walraven, F. (1977). The transition from the Transvaal Sequence to the Waterberg Group. *Transactions of the Geological Society of South Africa*, **80**, 145-146.

Compston, W., Williams, I.S., Kirschvink, J.L., Zang, Z. and Ma, G. (1992). Zircon U-Pb ages for the Early Cambrian timescale. *Journal of the Royal Geological Society, London*, **149**, 171-184.

Compston, W., Williams, I.S. and Myer, C. (1984). U-Pb geochronology of zircons from Breccia 73217 using a sensitive high mass-resolution ion microprobe. *Journal of Geophysical Research, Supplement*, **89**, B525-B534.

Cornell, D.H., Armstrong, R.A. and Walraven, F. (1998). Geochronology of the Proterozoic Hartley basalt Formation, South Africa: constraints on the Kheis tectogenesis and the Kaapvaal Craton's earliest Wilson cycle. *Journal of African Earth Sciences*, **26**, 5-27.

Crockett, R.N. and Jones, M.T. (1975). Some aspects of the geology of the Waterberg System in eastern Botswana. *Transactions Geological Society of South Africa*, **78**, 1-10.

Cumming, G.L. and Richards, J.R. (1975). Ore lead isotope ratios in a continuously changing Earth. *Earth and Planetary Science Letters*, **28**, 155-171.

de Bruyn, H. and Andrew, G.F. (1972). Syn-Waterberg volcanism in the vicinity of Rust de Winter dam. *Annals of the Geological Survey of South Africa*, **9**, 89-90.

de Kock, M.O., Evans, D.A.D., Dorland, H.C., Beukes, N.J. and Gutzmer, J. (2006) Paleomagnetism of the lower two unconformity-bounded sequences of the Waterberg Group, South Africa: Towards a better-defined apparent polar wander path for the Paleoproterozoic Kaapvaal Craton. *South African Journal of Geology,* **109**, 157-182.

Dorland, H.C. (2004). Provenance ages and timing of sedimentation of selected Neoarchean and Paleoproterozoic successions on the Kaapvaal Craton. Unpublished PhD thesis, Rand Afrikaans University, Johannesburg, South Africa, 326pp.

Du Toit, M.C. (1979). Die geologie en struktuur van die gebiede Levubu en Bandelierkop in Noord-Transvaal. *Unpublished Ph.D. thesis, Rand Afrikaans University, Johannesburg, South Africa*, 241pp.

Evans, D. A. D., Beukes, N. J. and Kirschvink, J. L. (2002). Paleomagnetism of a lateritic paleoweathering horizon and overlying Paleoproterozoic red beds from South Africa: Implications for the Kaapvaal apparent polar wander path and a confirmation of atmospheric oxygen enrichment. *Journal of Geophysical Research*, **107(B12)**: 2326-2333.

Glatthaar, C.W. (1956). Die verysterde piroklaste en 'n na-Waterbergse graniet suidoos van die dam Rust de Winter. *Unpublished MSc thesis, University of Pretoria, South Afric*a, 80pp.

Gutzmer, J. and Beukes, N.J. (1998). High grade manganese ores in the Kalahari manganese field: Characterisation and dating of the ore-forming events. *Unpublished Report, Rand Afrikaans University, Johannesburg, South Africa*, 221pp.

Hanson, R.E., Gose, W.A., Crowley, J.L., Ramezani, J., Bowring, S.A., Bullen, D.S., Hall, R.P., Pancake, J.A. and Mukwakwami, J. (2004). Paleoproterozoic intraplate magmatism and basin development on the Kaapvaal Craton: Age, paleomagnetism and geochemistry of ~1.93 to ~1.87 Ga post-Waterberg dolerites. *South African Journal of Geology*, **107**, 233-254.

Hartzer, F.J. (2000). Geology of Transvaal inliers in the Bushveld Complex. *Memoir of the Council for Geoscience, South Africa*, **88**, 222 pp.

Hisada, K. and Miyano, T. (1996). Petrology and microthermometry of aluminous rocks of the Botswana Limpopo Central Zone: evidence or isothermal decompression and isobaric cooling. *Journal of Metamorphic Geology*, **14**, 183-197.

Holzer, L., Barton, J.M., Paya, B.K. and Kramers, J.D. (1999). Tectonothermal history of the western part of the Limpopo Belt: tectonic models and new perspectives: *Journal of African Earth Sciences*, **28**, 383-402.

Holzer, L., Frei, R., Barton, J.M., and Kramers, J.D. (1998). Unravelling the record of successive high grade events in the Central-zone of the Limpopo Belt using single phase dating of metamorphic minerals. *Precambrian Research*, **87**, 87-115.

Jaeckel, P., Kröner, A., Kamo, S.L., Brandl, G. and Wendt, J.I. (1997). Late Archean to early Proterozoic granitoid magmatism and high-grade metamorphism in the central Limpopo belt, South Africa. *Journal of the Royal Geological Society. London*, **154,** 25-44.

Jansen, H. (1970). Volcanic rocks and associated sediments in the southern portion of the Waterberg basin. *Annals of the Geological Survey of South Africa*, **8**, 53-62.

Jansen, H. (1976). The Waterberg and Soutpansberg Groups in the Blouberg area, northern Transvaal. *Transactions of the Geological Society of South Africa*, **79**, 281-291.

Jansen, H. (1982). The geology of the Waterberg basins in the Transvaal, Republic of South Africa. *Memoir of the Geological Survey of South Africa*, **71**, 98pp.

Kamo, S.L., Reimold, W.U., Krogh, T.E. and Colliston, W.P. (1996). A 2.023 Ga age for the Vredefort impact event and a first report of shock metamorphosed zircons in pseudotachylitic breccias and granophyre. *Earth and Planetary Science Letters*, **144**, 369-388.

Key, R.M. (1983). The geology of the area around Gaborone and Lobatse District. *Memoir of the Geological Survey of Botswana*, **5**, 230pp.

Kröner, A., Jaeckel, P., Brandl, G., Nemchin, A.A. and Pidgeon, R.T. (1999). Single zircon ages for granitoid gneisses in the Central Zone of the Limpopo Belt, Southern Africa and geodynamic significance. *Precambrian Research*, **93**, 299-337.

Mapeo, R.B.M., Armstrong, R.A. and Kampunzu, A.B. (2001). SHRIMP U-Pb zircon geochronology of gneisses from Gweta borehole, northeast Botswana: implications for the Palaeoproterozoic Magondi Belt in southern Africa. *Geological Magazine*, **138**, 299-308.

Mapeo, R.B.M., Ramokate, L.V., Armstrong, R.A. and Kampunzu, A.B. (2004). U-Pb zircon age of the upper Palapye group (Botswana) and regional implications. *Journal of African Earth Sciences*, **40**, 1-16.

Martini, J.E.J. (1998). The Loskop Formation and its relationship to the Bushveld Complex, South Africa. Journal of African Earth Sciences, 27, 193-222.

McCourt, S. and Armstrong, R.A. (1998). SHRIMP U-Pb zircon geochronology of granites from the Central Zone, Limpopo Belt, southern Africa: Implications for the age of the Limpopo Orogeny. *South African Journal of Geology*, **101**, 329-338.

Meinster, B. (1977). Discussion on H. Jansen: The Waterberg and Soutpansberg Groups in the Blouberg area, northern Transvaal. *Transactions of the Geological Society of South Africa*, **80**, 289-296.

Oosthuyzen, E.J. and Burger, A.J. (1964). Radiometric dating of intrusives associated with the Waterberg System. *Annals of the Geological Survey of South Africa*, **3**, 87-106.

S.A.C.S. (South African Committee for Stratigraphy), (1980). Stratigraphy of South Africa. Part 1. Lithostratigraphy of the Republic of South Africa, South West Africa/Namibia and the Republics of Bophuthatswana, Transkei and Venda. *Handbook of the Geological Survey of South Africa*, **8**, 690 pp.

Schaller, M., Steiner, O., Studer, I., Holzer, I., Herwegh, M. and Kramers, J.D. (1999). Exhumation of Limpopo Central Zone granulites and dextral continent-scale transcurrent movement at 2.0 Ga along the Palala Shear Zone, Northern Province, South Africa. *Precambrian Research*, **96**, 263-288.

Schweitzer, J.K., Hatton, C.J. and De Waal, S.A. (1995). Regional lithochemical stratigraphy of the Rooiberg Group, upper Transvaal Supergroup: A proposed new subdivision. S*outh African Journal of Geology*, **98**, 245-255.

Van Niekerk, H.S., Beukes, N.J. and Gutzmer, J. (1999). Post-Gondwana pedogenic ferromanganese deposits, ancient soil profiles, African land surfaces and paleoclimatic change on the Highveld of South Africa. *Journal of African Earth Sciences*, **29**, 761-781.

Walraven, F. (1981). The stratigraphic position of the post-Rooiberg sediments at Rust de Winter. *Annals of the Geological Survey of South Africa*, **15**, 37-41.

Walraven, F. (1997). Geochronology of the Rooiberg Group, Transvaal Supergroup, South Africa. *Economic Geology Research Unit Information Circular, University of the Witwatersrand, South Africa,* **316,** 21pp.

Walraven, F. and Hattingh, E. (1993). Geochronology of the Nebo Granite, Bushveld Complex. *South African Journal of Geology*, **96**, 31-41.

Walraven, F., Armstrong, R.A. and Kruger, F.J. (1990). A chronostratigraphic framework for the north-central Kaapvaal Craton, Bushveld Complex and the Vredefort structure. *Tectonophysics*, **171**, 23-48.

Williams, I.S. and Claesson, S. (1987). Isotopic evidence for the Precambrian provenance Caledonian metamorphism of high grade paragneisses from the Seve Nappes, Scandinavian Caledonides. II ion microprobe zircon U-Th-Pb, *Contributions to Mineralogy and Petrology*, **97**, 205-217.

Editorial handling: J. Gutzmer